Available online at www.sciencedirect.com

ScienceDirect

Procedia Structural Integrity 64 (2024) 1549–1556

Structural Integrity Procedia

www.elsevier.com/locate/procedia

SMAR 2024 – 7th International Conference on Smart Monitoring, Assessment and Rehabilitation of Civil Structures

Bond behavior between metallic and non-metallic bars and sustainable concrete: preliminary study

Maria Antonietta Aiello[a], Denny Coffetti[b], Luigi Coppola[b], Maria Milena Della Vecchia[c], Marianovella Leone[a], Annalisa Napoli[c]*, Simone Rapelli[b], Roberto Realfonzo[c], Vincenzo Romanazzi[a]

[a]*Department of Engineering for Innovation, University of Salento, S.P. 6 – Monteroni, Lecce 73100, Italy*
[b]*Department of Engineering and Applied Science, University of Bergamo, Via Galvani 2, Dalmine (BG) 24044, Italy*
[c]*Department of Civil Engineering, University of Salerno, Via Giovanni Paolo II, Fisciano (SA) 84084, Italy*

Abstract

The study presented in the paper deals with the development and the characterization of an innovative shrinkage-compensating high-workability alkali activated slag-based eco-concrete for the repair and strengthening of reinforced concrete (RC) members. Furthermore, after the characterization of developed mixture at both fresh and hardened state, the paper focuses on the bond behavior between the new concrete and metallic and non-metallic (fiber reinforced polymer – FRP) rebars with the aim to: *a)* identify the main parameters influencing the stress transfer mechanisms at the interface and, *b)* to evaluate the bond-slip constitutive relationship by varying the steel bar diameter, the bonded length and, in the case of FRP bars, the surface treatment. To this purpose, a wide experimental program was organized which includes more than 100 pull-out tests performed on several types of rebars bonded to the new concrete and the preliminary results are presented here. The bond performance is also examined through a comparison with the results from similar tests performed by employing ordinary Portland cement concrete blocks characterized by equivalent compressive strength and workability class of the innovative green concrete.

Keywords: Bond; Cement – free concrete; FRP bars; Pull-out tests; Sustainability

* Corresponding author. Tel.: +39-089-964212.
E-mail address: annapoli@unisa.it

10.1016/j.prostr.2024.09.408

1. Introduction

Steel is the worldwide most used material as an internal reinforcement in reinforced concrete (RC) structures, due to its excellent mechanical properties, such as high tensile strength and elastic modulus as well as highly ductile behaviour. On the other hand, as a metallic material, it is prone to produce rust, being the corrosion an electrochemical process that involves the flow of electrons on the reinforcement surface.

Fiber reinforced polymer (FRP) bars represent one of the possible solutions to the problem of steel corrosion in RC structures because, being they electrochemical transparent, they cannot develop the electrochemical reactions leading to rust formation. Moreover, low weight, high tensile strength, wear resistance, enhanced fatigue life and low thermal expansion are further features that make FRP materials well-appreciated for the internal strengthening in RC structures as well as the external one for the upgrade of existing structures.

Sustainability is the nowadays great matter that involves all the scientific fields, including the building industry, in which this purpose can be achieved in different ways. One of them is the employment of FRP bars, which is widely less environmental impactful for two main reasons: their production process (less pollutant than the steel one) and enhanced resistance to adverse conditions thus delaying the need of maintenance interventions.

On the other hand, sustainability can be reached in the field of concrete too. The currently worldwide most used concrete is the Portland cement-based one, which production process is highly energy-intensive and requires the consumptions of large amounts of natural resources. The substitution of Portland cement as a binder in the concrete production is one of the possible suitable solutions to overcome these issues, hence ground granulated blast furnace slag (GGBFS) as an alternative binder is herein proposed. Due to its similar composition to Portland cement and good availability, blast furnace slag, which is a by-product of the cast-iron production process, is a good alternative binder, since its disposal is a significant concern too. Therefore, the use of slag in concrete may represent a step forward for many reasons: the reuse of waste materials and less consumption of energy and raw materials.

This paper presents the first results of a wide experimental study devoted to investigating the properties and performances of the FRP bars and “green concrete” untraditional materials. In particular, the experimental program involves research teams from three universities, i.e.: the University of Bergamo (UniBg), focused on the development and characterization of the green concrete, the University of Salento (UniSal) and University of Salerno (UniSa), both focused on the investigation of bond mechanism between FRP bars and green concrete. To this purpose, the paper presents the outcomes of the first performed direct pull-out tests. The results are presented in terms of bond stress (τ) vs slip (s) experimental curves, bond strength and failure type; comparisons with identical tests performed by using concrete made of ordinary Portland cement – namely “ordinary concrete (OC)” – are also discussed.

Nomenclature

f_{cm}	mean concrete cylindrical compressive strength
F	load
F_{max}	maximum load achieved
$F_{max,av}$	mean value of maximum load achieved in identical specimens
$F_{u,80\%}$	80% of maximum load
$F_{u,80\%,av}$	mean value of 80% of maximum load
L_b	bond length
R_{cm}	mean concrete cubic compressive strength corresponding to the day of pull-out test
s_{max}	free-end slip corresponding to the maximum load achieved
$s_{max,av}$	mean value of free-end slip corresponding to the maximum load achieved in identical specimens
$s_{u,80\%}$	free-end slip corresponding to 80% of maximum load
$s_{u,80\%,av}$	mean value of free-end slip corresponding to 80% of maximum load achieved in identical specimens
Ø	bar diameter
τ	bond stress
τ_{max}	maximum bond stress achieved
$\tau_{max,av}$	mean value of maximum bond stress achieved in identical specimens

2. Development and characterization of the "green concrete (GC)"

The first part of the research was aimed at the development and characterization of an innovative shrinkage-compensating, high-workability alkali-activated slag-based eco-concrete designed for the repair and reinforcement of RC structures. A blend of commercial ground granulated blast furnace slag and silica fume were activated with a solid precursor composed by sodium metasilicate, potassium hydroxide and sodium silicate to obtain a Portland-free sustainable binder (Coffetti et. al 2023, Komkova et al. 2023). Natural siliceous sands and gravels with maximum size of 12 mm were properly combined to meet the modified Bolomey granulometric curve. Moreover, due to the high susceptibility of alkali-activated materials to crack (Zhang et al. 2023 and Ye et al. 2016), 12 mm polypropylene fibers (shape index of about 400) were added to the mix for the prevention of plastic shrinkage cracking while CaO-based expansive agent and ethylene glycol-based shrinkage reducing admixture (SRA) were used to obtain a shrinkage-compensating material (Coppola et al. 2020). Finally, viscosity modifiers (methylcellulose and modified starch) were employed to ensure an adequate rheology of fresh concrete and a commercial superplasticizer containing modified acrylic polymers was selected to improve the workability and manage the setting time of green concrete. The water-to-binders ratio was fixed at 0.44 as indicated in the composition reported in Table 1.

To properly compare the bond of green and traditional concrete with reinforcements (Yan et al. 2016), the reference concrete was designed with the same aggregates used in alkali activated concrete to obtain similar workability (> 650 mm at flow table test) and 28-day compressive strength (> 45 MPa). As reference material, a flowable Portland-based shrinkage-compensating concrete was selected, using 400 kg/m^3 of a commercial premixed binder containing also superplasticizers, expansive agents and shrinkage reducing admixture in powder form. The water content was set to obtain a water-to-binder ratio of 0.46.

Different types of samples were produced and cured in a climatic chamber at 20°C and R.H. 95%: 100 mm cubes to evaluate the compressive strength at different ages and 150 mm cubes with embedded steel or FRP bars for the characterization of bond behavior. For the latter ones, the bond length of rebars with concrete was guarantee by the application of plastic tubes on the steel and FRP bars.

Table 1. Composition of green concrete

Components		Dosage [kg/m^3]
Precursors	Ground granulated blast furnace slag	450
	Silica Fume	60
Activators	Sodium metasilicate	71.6
	Potassium hydroxide	30.7
	Sodium Carbonate	10.2
Aggregates	Sand	995
	Gravel	405
Admixtures	Methylcellulose	0.56
	Modified starch	0.19
	SRA	6.75
	Expansive agent	13.5
	Superplasticizer	4.5
Polypropylene fibers		1
Tap water		198

3. Pull-out test

3.1. Experimental program

The whole experimental program includes 140 pull-out tests on reinforcing bars embedded into concrete cubes with 150 mm side; of these tests, 68 will be carried out at UniSal, while the remaining (72) ones at UniSa.

To examine the bond mechanism, the following main parameters were considered in the experimental program:

- the concrete type: ordinary concrete (OC) and green concrete (GC)
- the material of reinforcing bar: steel (S) and glass (G)FRP;
- the type of GFRP bar: G1 bar, supplied by Owens Conring® Pinkbar (2023) and G2 bar which were provided by Schöck Combar® (2023).
- the nominal bar diameter (Ø): Ø8 and Ø12;
- the bonded length of bar (L_b) within the concrete block: L_b = 2.5Ø or 5Ø.

Details about the test matrix are reported in Table 2 in which the values of both the core diameter and exterior diameter (core diameter + ribs thickness) are also reported; furthermore, the last two columns of the table report information about tests presented in this paper. In particular, these tests are 19 of which 13 were performed at UniSa and 6 at UniSal, all entailing Ø12 bars with L_b = 5Ø; 5 specimens were produced with GC and reinforced with steel bars (2 tests at UniSal and 3 at UniSa), while 14 cubes were made of OC, of which 7 reinforced with S bars and 7 with G1 bars (2+2 test at UniSal and 5+5 at UniSa).

Concerning the reinforcing bars, the deformed S ones were all of grade B450C steel, while the G1 bars were characterized by a 70% fiber mass content and by the following mechanical properties as reported in the technical sheet provided by the supplier (Owens Conring® Pinkbar 2023): tensile strength = 900 MPa, ultimate strain = 2%, modulus of elasticity = 46.88 GPa. Furthermore, to simulate the typical bond behavior between concrete and deformed steel bars, the G1 bars were characterized by the addition of ribs on the bar surface which were accurately measured before testing; in particular, the width and the thickness of these ribs – 6 mm spaced – were 5 and 0.25 mm.

Table 2. Test matrix.

Concrete type	Bar material	Nominal bar diameter, Ø (mm)	Core diameter (mm)	Exterior diameter (mm)	Bond length, Ø	# of planned tests		# of tests under investigation	
						UniSal	*UniSa*	*UniSal*	*UniSa*
Green (GC)	Steel (S)	12	12	12.8	2.5Ø	5	5	-	-
					5Ø	5	5	2	3
		8	8	9	5Ø	2	3	-	-
	FRP (G1)	12	12.7	13.2	2.5Ø	3	5	-	-
					5Ø	3	5	-	-
		8	8	8.5	5Ø	5	5	-	-
	FRP (G2)	12	12	13.5	2.5Ø	3	-	-	-
					5Ø	3	3	-	-
		8	8	9	5Ø	-	5	-	-
Ordinary (OC)	Steel (S)	12	12	12.8	2.5Ø	5	5	-	-
					5Ø	5	5	2	5
		8	8	9	5Ø	2	3	-	-
	FRP (G1)	12	12.7	13.2	2.5Ø	5	5	-	-
					5Ø	5	5	2	5
		8	8	8.5	5Ø	5	5	-	-
	FRP (G2)	12	12	13.5	2.5Ø	5	-	-	-
					5Ø	5	3	-	-
		8	8	9	5Ø	2	5	-	-

3.2. Set-up

The test setup, shown in Fig. 1a, was basically the same for both laboratories at UniSa (Fig. 1b) and UniSal (Fig. 1c); it was designed drawing inspiration from the RILEM Recommendations (1983).

The concrete samples were cubes with 150 mm side and were always casted in the same direction, i.e., orthogonally to the reinforcing bar (Fig. 1d); each bar was centrally embedded within the sample so that the concrete cover was higher than 4.5Ø. The chosen bonded length, equal to 5Ø for the tests discussed here, was consistent with the assumption of uniform distribution of the bond stress in the estimate of the bond stress (Eligehausen 1982). As shown in Fig. 1a, it was in the lowest part of the cube because, during the test, the compression stresses due to the steel plate exert a confinement action on the concrete which can enhance bond mechanism and, consequently, affect the test results. Thus, the chosen condition is as worst as possible for the bond, with the purpose to get more trustworthy results. The unbonded zone was realized by applying a plastic tube on the specific length of the bars (Fig. 1d).

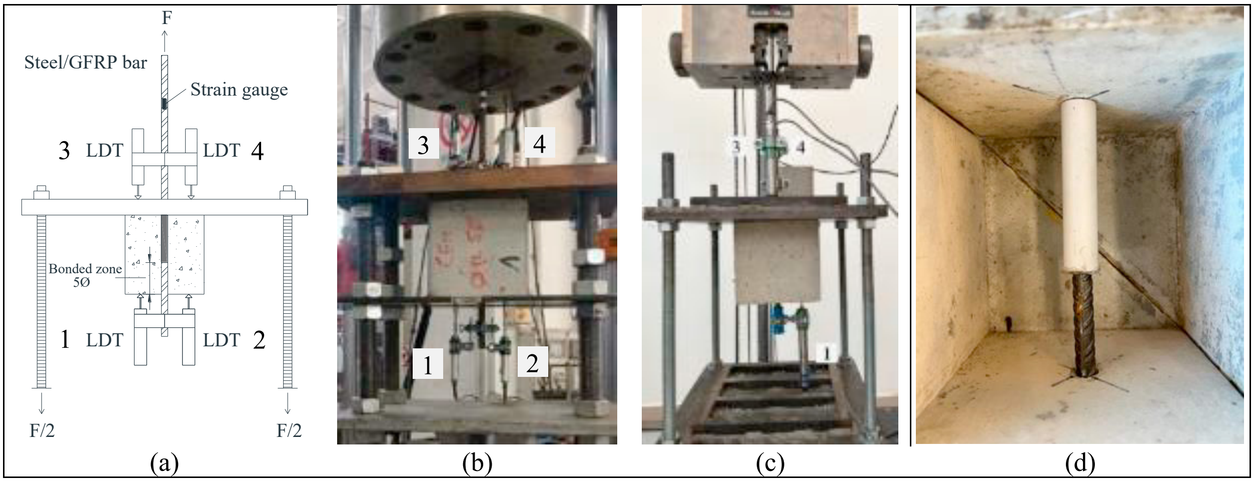

Figure 1. Pull-out test set-up (a); specimen before the pull-out test in UniSa Lab (b) and UniSal lab (c); casting direction (d).

Three or four LDTs (Linear Displacement Transducers) were used during tests: two attached at the unloaded end of the bar, while the other two (or one) were placed at the loaded end to measure the corresponding slips. Additionally, a strain gauge was glued directly onto the reinforcement bar to monitor its deformation throughout the testing phase.

The testing procedure involved the application of a tensile force using a displacement-controlled testing machine at a rate of 0.2 mm/min. All tests were stopped when a free slip of about 15 mm was reached.

4. Test results

Table 3 summarizes the main data and results of the 19 pull-out tests performed so far, i.e.:

- the university lab in which the test was performed;
- the test ID;
- the label related to the concrete casting;
- the age of concrete specimen at the test day;
- the mean value of the cubic compressive strength estimated at the test day (R_{cm});
- the maximum tensile load experienced by each specimen during the test (F_{max}) and the corresponding mean value calculated for each set of identical specimens ($F_{max,av}$) together with the corresponding coefficient of variation, CoV (reported in round brackets);
- the interface bond strength· $\tau_{max} = F_{max}/(\pi \cdot \phi \cdot L_b)$ calculated for the specimen and the corresponding free-end slip (s_{max});
- the mean values of τ_{max} and s_{max} obtained for each set of identical specimens ($\tau_{max,av}$, s_{max}), together with the CoV value calculated for s_{max} (reported in round brackets);
- the ultimate force calculated at both 80% strength decay evaluated on the load-free end slip curve and the corresponding slip values (i.e., $F_{u,80\%}$ and $s_{u,80\%}$);
- the mean values of $s_{u,80\%}$ and the corresponding CoV values (reported in round brackets) calculated for each set of identical specimens.

The test ID in Table 3 provides the following information: a) the number following "OC" provides information about the concrete casting to which the specimen belongs (GC or OC, from OC1 to OC4), b) the reinforcing bar material (S or G1). About the concrete casting, it is highlighted that the 5 specimens made of GC and tested so far were cast all together, while the 14 OC cubes were cast in four different casting times, indicated in Table 3 with labels going from OC1 to OC4.

Concerning the slip data, instead, it is noted that values of the free-end slip of the bar reported in Table 3 represent the average of the measures directly provided by the LDT 1 and LDT 2 illustrated in Figure 1b for UniSa and the slip recorded by LDT1 in Fig. 1c for UniSal. Conversely, the values of the slip at the loaded end of the bar, omitted in Table 3 for brevity, can be derived from the average of the measures provided by LDT 3 and LDT 4 in Fig. 1b and

1c, for both universities. These measurements must be pre-adjusted to account for the elastic elongation of the bar between the top side of the concrete cube and the anchor system of the LDTs.

Table 3. Main data and test results

Lab	ID Specimen	Concrete type	Age of test [days]	R_{cm} [MPa]	F_{max} [kN]	$F_{max,av}$ [kN]	τ_{max} [MPa]	$\tau_{max,av}$ [MPa]	s_{max} [mm]	$s_{max,av}$ [mm]	$F_{u,80\%}$ [kN]	$s_{u,80\%}$ [mm]	$s_{u,80\%,av}$ [mm]
UniSa	GC_S_1	GC	28	43.7	32.4	29.99 (11.46%)	14.3	13.3	0.54	0.52 (5.06%)	25.9	1.87	2.08 (14.28%)
	GC_S_2	GC	28	43.7	27.6		12.2		0.50		22.1	2.29	
	GC_S_3	GC	50	48.2	34.8	-	15.4	-	0.80	-	27.8	2.33	-
UniSal	GC_S_1	GC	130	*50.0**	38.6	40.6 (6.80%)	17.1	17.9	0.55	0.51 (12.60%)	30.7	2.29	2.30 (0.61%)
	GC_S_2	GC	130	*50.0**	42.5		18.8		0.46		34	2.31	
UniSa	OC1_S_1	OC1	50	47.1	26.2	30.55 (15.44%)	11.6	13.5	0.96	0.70 (42.82%)	20.9	1.96	2.06 (12.84%)
	OC1_S_2	OC1	50	47.1	30.0		13.2		0.79		24.0	2.36	
	OC1_S_3	OC1	50	47.1	35.5		15.7		0.37		28.4	1.96	
	OC4_S_4	OC4	28	50.9	42.0	43.43 (4.72%)	18.6	19.2	0.88	1.03 (20.60%)	33.6	2.58	2.8 (11.11%)
	OC4_S_5	OC4	28	50.9	44.9		19.8		1.18		35.9	3.02	
UniSal	OC1_S_1	OC1	135	*50.6**	38.5	41.0 (8.62%)	17.0	18.1	1.00	0.91 (13.99%)	30.83	3.02	2.67 (18.84%)
	OC1_S_2	OC1	135	*50.6**	43.5		19.2		0.82		34.8	2.31	
UniSa	OC2_G1_1	OC2	50	52.0	35.0	36.11 (4.35%)	14.6	15.1	2.43	2.34 (5.75%)	28.0	4.17	4.17 (0.17%)
	OC2_G1_2	OC2	50	52.0	***20.5***		***8.5***		***1.46***		16.4	***2.42***	
	OC2_G1_3	OC2	50	52.0	37.2		15.6		2.24		29.8	4.16	
	OC3_G1_4	OC3	32	52.4	33.0	33.43 (1.93%)	13.7	14.0	1.63	1.70 (5.82%)	26.4	3.55	3.44 (4.52%)
	OC3_G1_5	OC3	32	52.4	33.9		14.2		1.77		27.1	3.33	
Unisal	OC2_G1_1	OC2	132	51.4	44.9	43.3 (5.40%)	18.8	18.1	2.58	2.56 (1.38%)	36.0	4.30	4.33 (0.82%)
	OC2_G1_2	OC2	132	51.4	41.6		17.4		2.53		33.3	4.35	

** Analytically estimated according to EC2 (2005); values in bold are not included in the average of results for the corresponding set*

All the specimens exhibited a pull-out failure since the bar was pulled out from the cube without any visible damage on concrete cover.

Fig. 2 shows comparisons in terms of bond stress versus free-end slip *(τ-s)* curves for identical tests performed in the two involved universities. In particular, Fig. 2a and 2b show the comparison between the bond performances exhibited by ordinary concrete and green concrete when the reinforcing bar is made of steel; Fig. 2 (c) and (d), instead, show, in the case of OC, the comparison in terms of bond performance between steel and GFRP bars.

In the case of GC and OC with steel bar (Fig. 2a and 2b), the experimental behaviors of identical samples performed in the two laboratories are quite comparable. The *(τ-s)* curves are characterized by an initial ascending branch in which the first part is governed by the chemical adhesion while for the remaining one the mechanical interlocking governs the bond behavior. In the first stage, when the steel-concrete stresses transfer mechanism is given by the chemical adhesion, the relative slips are almost zero. Once the chemical adhesion is overcome, a diffuse micro-cracking in the steel-concrete happens in the interfacial transition zone and the slip increases.

In this second stage, the transfer mechanism is driven by the mechanical interlocking. After the attainment of the peak bond stress and the subsequent stress decay, a horizontal residual stress plateau is observed. In this case, similar bond strength values have been obtained for GC and OC1 with steel bars, despite a slightly difference in s_{max} values.

A barely significant difference between the two kinds of concrete was observed in the final branch of the bond stress – slip curves, in which it has been observed a slightly higher residual bond strength shown by green concrete; probably, this is due to the higher porosity of GC that can improve bond performances (Romanazzi et al. 2022).

Conversely, the differences between traditional steel bars and FRP bars are more significant than those already seen in the comparison between conventional and unconventional concrete (Fig. 2c and 2d). In this case, indeed, the bond stress – slip law obtained by tests performed on samples reinforced with steel bars is clearly stiffer than that corresponding to tests carried out on GFRP bars. This is due to the different bond mechanism developed by the two kinds of concrete, which is ruled by the same contributions, even though in varying degrees.

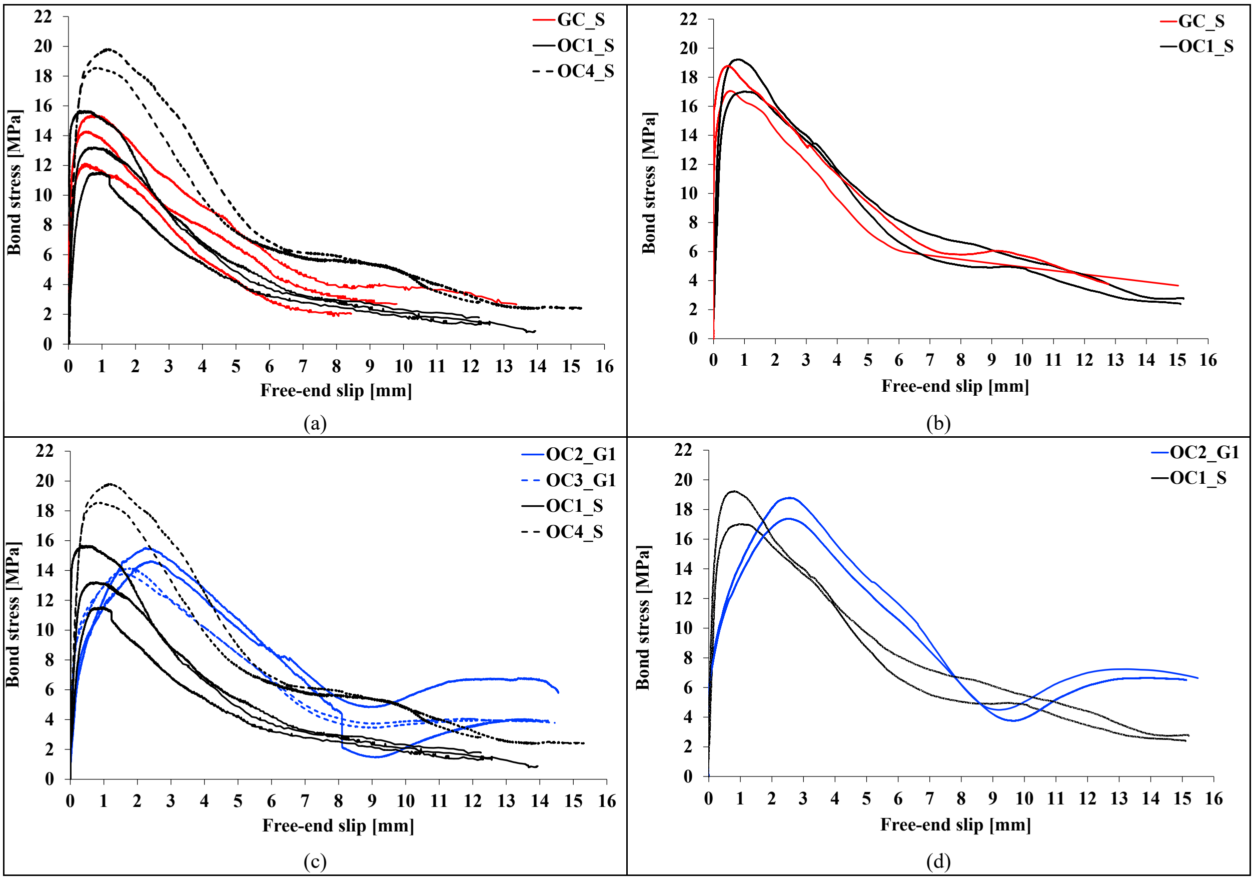

Figure 2. Bond stress versus free-end slip curve: comparison between GC and OC (a,b) and between steel and GFRP bars (c,d) for tests performed at UniSa (a,c) and UniSal (b,d).

Overall, the curves obtained for the ribbed GFRP bars have the same shape as the curves for steel bars. Despite a very similar bond strength, the different bond stiffness from the chemical adhesion failure (i.e., zone with no slip) to the maximum bond stress appears evident from the graphs. This is also confirmed from Table 3 where the slip values s_{max} corresponding to the bond strength measured in the case of steel bars are about 64% (UniSal) and 57% (UniSa) lower than those recorded with G1 bars. Up to the achievement of the peak stress, the bond mechanism is governed by the mechanical interlocking and, according to Metelli et al. (2014), the bond stiffness of this branch is directly linked with the rib's geometry. In this case, it is evident that the ribs of the deformed steel bars provide a more efficient interlocking with the surrounding concrete than the G1. In fact, ribs on GFRP bars surface are mainly made of matrix, which is much less resistant than steel. Consequently, once chemical adhesion is won, mechanical interlocking becomes the ruling contribute to bond mechanism, but it developed in varying degrees in samples reinforced with steel or GFRP bars, since being steel ribs stronger, they were able to retain concrete. The same cannot be said for GFRP bars, in which ribs got smoothed during the test and could not hold concrete on their surface. Once high displacements were reached during the test, friction was the only contribute to bond and, once again, differences between steel and GFRP bars were observed, because in the first case friction is concrete – to – concrete, while in the latter it develops between concrete and GFRP bar. This is why, in GFRP reinforced specimens, a sudden increase of bond stress during the frictional stage has been observed, probably due to the contribution of an intact rib.

5. Conclusions

In this paper, the first results of a wide experimental program devoted to investigating the bond mechanism between sustainable concrete and metallic or non-metallic (GFRP) reinforcing bars were presented. The study is part of a broader project involving research teams from the University of Bergamo (UniBg), University of Salento (UniSal) and University of Salerno (UniSa), aimed at developing a new cement-free concrete for structural purposes.

The sustainable concrete was developed and mechanically characterized by UniBg's research team. It was obtained by replacing Portland cement with an alternative binder made of ground granulated alkali-activated blast furnace slag, a by-product of cast iron production.

The bond performance between the new concrete and the reinforcing bars in under investigation by both UniSa and UniSal research teams. To date, 19 direct pull-out tests have been performed and, among them, 13 at UniSa Laboratory and 6 at the UniSal Laboratory. For a better understanding, the bond performance was examined by comparing the results obtained with those derived from identical pull-out tests using ordinary Portland cement-based concrete and the same was done by comparing GFRP reinforced samples behavior to those reinforced with steel bars. Bond length and nominal bar diameter were respectively equal to 5Ø and Ø12, for each tested specimen.

The following main observations were made:

- negligible dissimilarities in bond mechanism developed in specimens made of ordinary or green concrete were observed, except for residual bond strength which resulted higher in green concrete;
- samples reinforced with steel bars and GFRP bars showed comparable bond strength but dissimilar behavior, since the latter showed higher slip than the first ones;
- unlike steel bars, it was seen that GFRP bars were not able to hold concrete among ribs since they got smoothed during the test. This means that, even though bond mechanism is ruled by the same contributions, they behave in different ways and degree.

Acknowledgements

The research was carried out with the financial support from ReLUIS (Network of the Italian University Laboratories for Seismic Engineering—Italian Department of Civil Protection) - Executive Project 2022–24—WP14.
The authors thank Owens Corning (Toledo, Ohio, USA) and Schöck Italia GmbH S.r.l. (Bolzano, Italy) for providing the GFRP bars used in the experimental investigation.

References

Coffetti, D., Candamano S., Crea, F., Coppola, L., 2023. On the rote of alkali content on one-part alkali activated slag pastes produced with tri-blend solid activators. Constr. Build. Master 409.

Coppola, L., Coffetti D., Crotti S., Candamano S., Crea F., Gazzaniga, G., Pastore, T., 2020. The combined use of admixtures for shrinkage reduction in one-part alkali activated slag-based mortars and pastes, 2020. Constr. Build. Master. 248.

Eligehausen, R., Popov, E. P., Bertero, V. V., 1982. Local Bond Stress-Slip Relationships of Deformed Bars Under Generalized Excitations. 4, 69-80

EN 1992-2 2005. Eurocode 2: Design of concrete structures.

Komkova, A., Habert, G., 2023. Environmental impact assessment of alkali-activated materials: Examining impacts of variability in constituent production processes and transportation, 2023. Constr. Build. Master 363.

Metelli, G., Plizzari, G. A., 2014. Influence of the relative rib area on bond behaviour. Mag. Concr. Res. 66, 277-294

Owens Corning website. https://www.owenscorning.com/en-us/composites/product/flatworkfiberglassrebar (Accessed 10 December 2023).

RILEM TC, RC 6, 1983. Bond test for reinforcement steel. 2. Pull-out test.

Romanazzi, V., Leone, M., Aiello, M.A., Pecce, M.R., 2022. Bond behavior of geopolymer concrete with steel and GFRP bars. Compos. Struct. 300, 116150.

Schöck website. https://www.schoeck.com/en/combar. (Accessed 10 December 2023).

Taha, N. A., Morsy, M., 2014. Study of the behavior of corroded steel bar and convenient method or repairing. Housing and Building National research Center Journal 12, 107-113.

Yan, F., Lin, Z., Yang M., 2016. Bond mechanism and bond strength of GFRP bars to concrete: A review. Compos. Part B Eng. 98, 56-69.

Ye, H., Radlińska, 2016. Shrinkage mechanisms of alkali-activated slag.

Zhang W., Xue, M., Lin H., Jin Y., Su, F., 2023. Effect of polymer shrinkage reducing admixture on the drying shrinkage properties of alkali-activated slag. Cem. Concr. Compos 136.